



Original Articles

MDM2-NFAT1 dual inhibitor, MA242: Effective against hepatocellular carcinoma, independent of p53



Wei Wang^{a,b,*,1}, Jian-Wen Cheng^{c,d,1}, Jiang-Jiang Qin^{a,1}, Bo Hu^{c,d}, Xin Li^a, Bhavativya Nijampatnam^e, Sadanandan E. Velu^e, Jia Fan^c, Xin-Rong Yang^{c,***}, Ruiwen Zhang^{a,b,*}

^a Department of Pharmacological and Pharmaceutical Sciences, College of Pharmacy, University of Houston, Houston, TX, 77204, USA

^b Drug Discovery Institute, University of Houston, Houston, TX, 77204, USA

^c Department of Liver Surgery & Transplantation, Liver Cancer Institute, Zhongshan Hospital, Fudan University, Shanghai, China

^d Key Laboratory of Carcinogenesis and Cancer Invasion of Ministry of Education, Zhongshan Hospital, Fudan University, Shanghai, China

^e Department of Chemistry, University of Alabama at Birmingham, Birmingham, AL, 35294, USA

ARTICLE INFO

Keywords:

Hepatocellular carcinoma
MDM2
NFAT1
Metastasis
CRISPR/Cas9
Patient-derived xenograft

ABSTRACT

The overexpression of the MDM2 oncoprotein frequently occurs in hepatocellular carcinoma (HCC). Small molecules that inhibit MDM2-p53 binding show efficacy against p53 wild-type HCC, but most patients have p53-mutant tumors and intrinsic resistance to such MDM2 inhibitors. We have recently discovered that the NFAT1 transcription factor upregulates MDM2 expression, but the role of NFAT1 in HCC is not fully understood. The present study was designed to develop a dual-targeting (MDM2 and NFAT1) strategy for the treatment of HCC. We herein demonstrate that high expression levels of NFAT1 and MDM2 are independent predictors of a poor prognosis in patients with HCC. We have also identified a MDM2 and NFAT1 dual inhibitor (termed MA242) that induces MDM2 auto-ubiquitination and degradation and represses NFAT1-mediated MDM2 transcription. MA242 profoundly inhibits the growth and metastasis of HCC cells *in vitro* and *in vivo*, independent of p53. The present efficacy and mechanistic studies provide proof-of-principle data to support the therapeutic value of this dual targeting strategy in future drug discovery.

1. Introduction

Hepatocellular carcinoma (HCC) represents a major public health burden, and is the third leading cause of cancer mortality worldwide [1]. Despite recent advances in the early diagnosis and treatment of HCC, most patients present with intermediate or advanced-stage disease, and the five-year survival rate remains unsatisfactory [2,3]. The knowledge regarding hepatocarcinogenesis has expanded significantly, allowing the identification of the molecular processes involved in the onset and progression of this neoplastic disorder. Growth factors, pro-angiogenic factors and their receptors, intracellular tyrosine kinase pathways and signal transmission factors have been identified as being particularly important [4–6]. However, the treatment options for advanced HCC are still limited [4–6]. Therefore, there is an urgent need to

develop safe and effective agents to treat patients with HCC, especially those with advanced disease.

The murine double minute 2 (MDM2) oncogene is highly expressed and frequently activated in many human cancers, including HCC [7–10]. MDM2 enhances cancer cell growth and cell cycle progression, prevents apoptosis, induces cell migration and invasion, regulates metabolism and inflammation, and desensitizes cells to chemotherapy via p53-dependent and -independent pathways [11–13]. Given the ubiquity of MDM2 and its critical roles in human cancer cells, we and other investigators have demonstrated that MDM2 is a promising molecular target for the development of new anticancer drugs [14,15]. Most small molecule inhibitors (SMIs) of MDM2 have been developed to disrupt the MDM2-p53 interaction, thus activating p53 signaling and inducing cancer cell apoptosis [16]. Several drug candidates based on this

* Corresponding author. Department of Pharmacological and Pharmaceutical Sciences, School of Pharmacy, University of Houston, 4849 Calhoun Rd, Houston, TX, 77204, USA.

** Corresponding author. Department of Pharmacological and Pharmaceutical Sciences, School of Pharmacy, University of Houston, 4849 Calhoun Rd, Houston, TX, 77204, USA.

*** Corresponding author. Liver Cancer Institute, Fudan University, 136 Yi Xue Yuan Road, Shanghai, 200032, China.

E-mail addresses: wwang4@central.uh.edu (W. Wang), yang.xinrong@zs-hospital.sh.cn (X.-R. Yang), rzhang27@central.uh.edu (R. Zhang).

¹ These authors contributed equally to this work.

strategy have entered clinical trials. However, the majority of HCC harbors mutated p53 [17,18] and thus presents intrinsic resistance to these MDM2-p53 interaction-targeting SMIs [19]. In addition, the p53-independent regulation of MDM2 has emerged as an important mechanism that controls its expression level in tumors, particularly late-stage and metastatic tumors [13]. Given its attractiveness as a candidate drug target, there is an urgent need to identify a strategy to target MDM2 that is not dependent on wild-type p53.

In addition to down-regulating p53, MDM2 interacts with or/and regulates numerous other proteins (e.g., pRb, histone acetyltransferases, steroid receptors) [13]. We have recently demonstrated that the Nuclear Factor of Activated T Cells 1 (NFAT1) directly binds to the P2 promoter of *mdm2* and induces its expression, leading to accelerated cell proliferation and resistance to apoptosis induced by DNA damaging agents [20]. Following its initial discovery in T lymphocytes [21], a multitude of studies have demonstrated that the NFAT1 protein is also expressed in cells outside the immune system, where it regulates a variety of biological processes [22–24]. NFAT1 promotes cancer cell growth, cell cycle progression, migration, invasion, and angiogenesis through calcineurin-dependent and -independent pathways, suggesting that NFAT1 has roles in cancer progression [24]. Recent studies have demonstrated that by calcineurin activity reduction and nuclear translocation of NFAT1 inhibition, regulator of calcineurin 1 isoform 4 (RCAN1.4) overexpression prevents cell growth, angiogenesis, and metastases in HCC [25]. In HCC immunotherapy, upregulated Lnc-Tim3 induces CD8 T cell exhaustion by reducing NFAT1 signaling pathway. At the same time, Lnc-Tim3 increases p53 acetylation and the expression of p21, MDM2, and Bcl-2 [26]. However, functions of NFAT1 itself in HCC development and progression remain unknown. In light of our recent findings [20], we hypothesized that the NFAT1-MDM2 pathway promotes hepatocarcinogenesis and that targeting this pathway would have therapeutic effects against HCC. Traditional NFAT1 inhibitors (e.g., CsA or tacrolimus) inhibit the dephosphorylation of numerous substrates, including NFAT and proteins associated with other signaling pathways, by interfering with calcineurin activity [24]. However, the lack of specificity of these inhibitors may result in diverse effects on the cellular pathophysiology and a high risk of off-target effects. In addition, most of these inhibitors have not been tested in cancer models, and there have been no specific NFAT1 inhibitors developed to date. Therefore, new strategies to specifically inhibit NFAT1 are urgently needed.

The present study was designed to demonstrate the role of the NFAT1-MDM2 pathway in hepatocarcinogenesis and to determine its translational potential for HCC therapy. We herein investigated the expression of MDM2 and NFAT1 in 254 pairs of human HCC and matched non-cancerous tissue samples, and demonstrated that a dual inhibitor of MDM2 and NFAT1, MA242, has potent effects against various models of HCC. We also explored the underlying mechanisms of action, with a focus on whether the effects require wild-type p53. The results of the present study provide a basis for the development of a dual-targeting (MDM2 and NFAT1) strategy for the treatment of HCC.

2. Materials and methods

More detailed information is provided in the *Supplemental Methods*.

2.1. Patients and specimens

Archived tissue samples for tissue microarray (TMA) construction were obtained from a consecutive cohort of 254 patients who underwent surgery for curative resection of HCC in the Liver Cancer Institute, Zhongshan Hospital, Fudan University (Shanghai, China) between January 1, 2006 and December 30, 2006. The conventional clinicopathological variables and their relationship with MDM2 and NFAT1 expression are provided in Table 1.

Table 1

The correlations between the MDM2 and NFAT1 expression levels and the clinicopathological features of HCC patients.

Characteristic	Cases	MDM2			NFAT1		
		Low	High	P value	Low	High	P value
Age (years)							
≤ 50	123	43	80	0.163	53	70	0.859
> 50	131	57	74		55	76	
Gender							
Male	206	77	129	0.178	87	119	0.848
Female	48	23	25		21	27	
HBSAg							
No	44	19	25	0.569	20	24	0.569
Yes	210	81	129		88	122	
Anti-HCV							
No	251	99	152	0.830	107	144	0.746
Yes	3	1	2		1	2	
AFP (ng/mL)							
≤ 40	136	63	73	0.015	62	74	0.288
> 40	118	37	81		46	72	
ALT (u/L)							
≤ 75	226	87	139	0.418	94	132	0.396
> 75	28	13	15		14	14	
γGT (U/l)							
≤ 54	97	39	58	0.830	47	50	0.133
> 54	157	61	96		61	96	
Tumor size (cm)							
≤ 5	144	65	79	0.031	63	81	0.650
> 5	110	35	75		45	65	
Tumor multiplicity							
Single	216	90	126	0.074	96	120	0.139
Multiple	38	10	28		12	26	
Tumor differentiation							
I-II	195	79	116	0.295	91	104	0.020
III-IV	55	18	37		16	39	
Vascular invasion							
Yes	164	77	87	0.001	82	82	0.001
No	90	23	67		26	64	
Tumor encapsulation							
Yes	142	59	83	0.423	65	77	0.237
No	112	41	71		43	69	
BCLC stage							
A + B	190	67	123	0.021	79	111	0.601
C + D	64	33	31		29	35	

Pearson's chi-squared test was used to determine the significance.

Abbreviations: HBsAg, hepatitis B surface antigen; anti-HCV, hepatitis C virus antibody; AFP, alpha-fetoprotein; ALT, alanine aminotransferase; γGT, gamma-glutamyl transferase; BCLC, Barcelona clinic liver cancer.

2.2. Tissue microarray, immunohistochemistry and hematoxylin and eosin (H&E) staining

Tissue microarrays were produced as described previously [27]. All HCC cases were histologically reviewed by HE staining, and representative tumor areas were pre-marked in the paraffin blocks, away from necrotic and hemorrhagic materials. The immunohistochemical and HE staining of serial TMAs was carried out as described previously [27].

2.3. Screening and characterization of new dual inhibitors of MDM2 and NFAT1

The new MDM2 and NFAT1 dual inhibitors, MA242 and analogs, were characterized using a three-step approach, including a computational 3D structure-based search for the identification of the pyrroloiminoquinone scaffold, structural design and synthesis [28]. They were then evaluated using biotin-MA242 pull-down assays [29], cellular thermal shift assays [30], and cell-based assays.

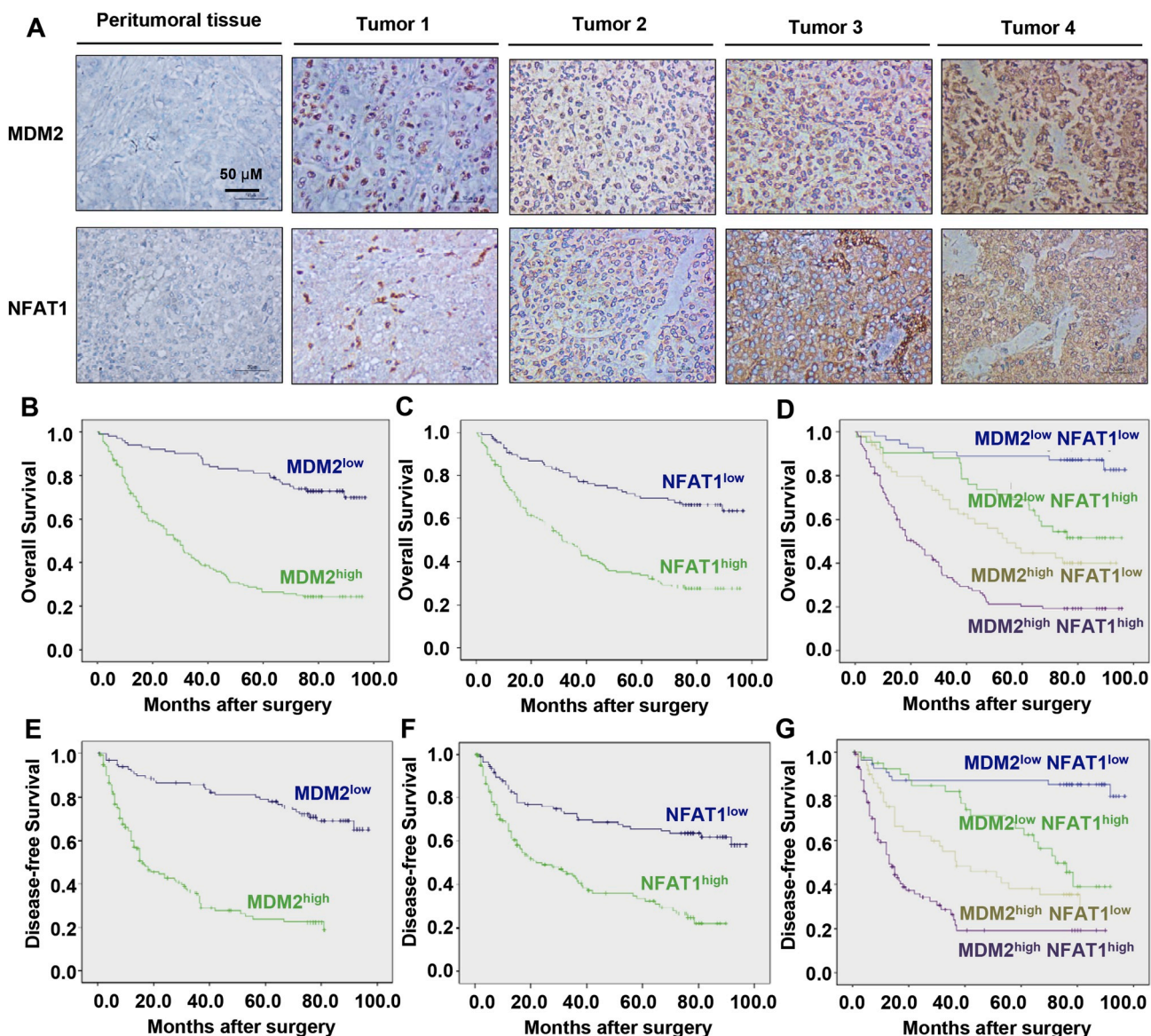


Fig. 1. MDM2 and NFAT1 are frequently overexpressed in HCC tissues, and high levels of MDM2 and NFAT1 are associated with a poor prognosis. (A) Representative images of the MDM2 and NFAT1 staining in tissue microarrays as determined by an immunohistochemical analysis (all images represent serial sections; scale bar, 50 μ m). (B, C, D) High levels of MDM2 and NFAT1 had a shorter overall survival (OS). The differences in the OS between 254 HCC patients with (B) high or low MDM2 expression; (C) high or low NFAT1 expression; and (D) different co-expression of MDM2 and NFAT1, as determined by a Kaplan–Meier analysis (log-rank test). (E, F, G) High levels of MDM2 and NFAT1 had a shorter recurrence-free survival (RFS). The RFS rates of the same cohort of HCC patients were compared between the (E) MDM2-low and -high groups; (F) high or low NFAT1 expression; and (G) co-expression of MDM2 and NFAT1. The Kaplan–Meier method (log-rank test) was used for the analyses.

2.4. Chemicals, antibodies, plasmids, cell lines and other reagents

All chemicals and solvents were of analytical grade. Antibodies, plasmids, and cell lines [31,32] were obtained commercially or were provided by other investigators. The route of biotin-MA242 synthesis and a detailed list of reagents are provided in the *Supplemental Methods*.

2.5. Establishment of CRISPR-Cas9 MDM2 KO constructs

Protospacer sequences of CRISPR/cas9 against MDM2 and GFP (control vector) were designed and constructed per a previous report [33]. The specific target sequences were amplified and cloned into lenti-CRISPR vectors and verified by DNA sequencing.

2.6. Assays of the *in vitro* anticancer activity of MA242

All of the assays used to determine the effects of MA242 on cell viability (MTT assay), colony formation, cell proliferation [bromodeoxyuridine (BrdU) incorporation assay], cell apoptosis (Annexin V-FITC apoptosis detection kit), cell cycle distribution, cell migration (wound healing assay), and cell invasion (transwell invasion assay) were performed as described previously [27–29].

2.7. Western blotting, real-time quantitative PCR, immunofluorescence, luciferase reporter assay

The protein and mRNA expression levels of MDM2 and other molecules were determined by Western blotting and real-time quantitative PCR, respectively [27–29]. Immunofluorescence staining was performed to determine the expression and location of the MDM2 protein

in the cells [27–29]. The *MDM2* promoter activity was determined using a luciferase reporter assay [34].

2.8. Ubiquitination assay

HCC cells were co-transfected with *MDM2* and ubiquitin plasmids and treated with MA242 for 24 h, then the cell lysates were collected and immunoprecipitated with an anti-*MDM2* antibody. The bound proteins were examined for *MDM2* ubiquitination using an anti-ubiquitin antibody [27–29].

2.9. Electrophoretic mobility shift assay (EMSA) and chromatin immunoprecipitation (ChIP)

EMSA and ChIP assays were performed to examine the NFAT1-*MDM2* P2 promoter complex as reported previously [20].

2.10. HCC xenograft, orthotopic, and patient-derived xenograft (PDX) tumor models and animal treatment

The animal protocols were approved by the Institutional Animal Use and Care Committee of University of Houston. The establishment of HCC xenograft models, orthotopic models and PDX models, and the evaluation of the tumor growth and clinical status of the mice, were performed as reported previously [27,35]. The protocols used for animal model development and treatment are described in detail in the *Supplemental Methods*.

2.11. Statistical analysis

The statistical analyses of all clinical data were performed with the SPSS 18.0 software program for Windows (IBM). For preclinical studies, the statistical analyses were performed using the Prism software, version 6 (Graph Pad Software Inc., San Diego, CA). Differences were considered statistically significant at $P \leq 0.05$. The details of the statistical analysis are described in the *Supplemental Methods*.

3. Results

3.1. High tumor expression of *MDM2* and *NFAT1* correlates with a poor prognosis in HCC patients

To determine the expression of the *MDM2* and *NFAT1* proteins in HCC and their clinical significance, tissue microarrays (TMAs) from 254 patients with HCC were examined by immunohistochemical staining (Fig. 1A). We found that 154 (60.6%) HCC cases had intense staining of *MDM2*, whereas 39.4% showed low *MDM2* expression. The overexpression of *MDM2* was significantly associated with a high alpha-fetoprotein (AFP) level ($P = 0.015$), large tumor size ($p = 0.031$), vascular invasion ($p = 0.001$) and a higher BCLC stage ($p = 0.021$) (Table 1), all of which are considered to indicate an aggressive clinicopathological course. To evaluate the prognostic significance of *MDM2*, the overall survival (OS) and recurrence-free survival (RFS) rates were analyzed. As expected based on the above-mentioned factors, patients with high *MDM2* expression had a significantly poorer OS and RFS than those with low *MDM2* expression (Fig. 1B and E). In univariate and multivariate analyses, the *MDM2* status was identified as an independent prognostic factor for both the OS and RFS (Tables S1 and S2).

After scoring, we observed that 146 (57.5%) HCC cases overexpressed *NFAT1*. The patients with high *NFAT1* expression were significantly more likely to have metastasis and aggressive tumors. *NFAT1* overexpression was significantly associated with tumor differentiation ($p = 0.020$) and vascular invasion ($p = 0.001$) (Table 1). The prognostic effect of *NFAT1* on the OS and RFS in patients with HCC was also assessed by univariate and multivariate analyses. Cox's regression

analysis showed that, compared with the tumors with low *NFAT1* expression, HCC patients whose tumors had a high level of *NFAT1* had a shorter OS and RFS (Fig. 1C and F). *NFAT1* was also identified as an independent prognostic factor for the OS and RFS in patients with HCC in univariate and multivariate analyses (Tables S1 and S2).

Interestingly, we found that *MDM2* and *NFAT1* were simultaneously overexpressed in many HCC patients. We therefore divided the HCC patients into four groups: *MDM2*^{high}/*NFAT1*^{high}, *MDM2*^{high}/*NFAT1*^{low}, *MDM2*^{low}/*NFAT1*^{high}, and *MDM2*^{low}/*NFAT1*^{low}. For the whole study population, the OS (and RFS) rates at one, three, five, and seven years post-hepatectomy were 68.7% (53.6%), 31.4% (24.0%), 20.3% (19.2%), and 19.2% (19.2%); 83.9% (75.2%), 64.8% (55.1%), 44.7% (38.2%), and 40.0% (28.4%); 90.5% (92.5%), 88.1% (82.1%), 69.0% (65.4%), and 51.1% (39.0%); and 96.4% (90.8%), 90.9% (87.1%), 89.1% (87.1%), and 87.3% (85.2%) respectively, for these four groups. Significant differences were found among all groups ($p < 0.001$), except for the comparison between *MDM2*^{high}/*NFAT1*^{low} and *MDM2*^{low}/*NFAT1*^{high} groups (Fig. 1D and G).

3.2. MA242 is a specific dual inhibitor of *MDM2* and *NFAT1*

We previously designed and synthesized a class of makaluvamine analogs by employing a structure-based approach (Fig. S1). MA242 (Fig. 2A) was identified as a potent and selective dual inhibitor of *MDM2* and *NFAT1*. Our molecular docking studies with the SYBYL-X program predicted that MA242 specifically binds to the C-terminal RING domain of *MDM2* (PDB ID: 2VJF) via key amino acid (aa) residues (HIS457 and LYS446) (Fig. 2A and B). The 2-amino group and 4-methylphenyl group of MA242 directly interact with HIS457 and LYS446 (respectively) via hydrogen bonding. To further examine the direct binding of MA242 to *MDM2*, we conjugated biotin with MA242 (Fig. 2C & S2) so that it could be used in a specific biotin-avidin pull-down assays. As shown in Fig. 2D, biotin-MA242 specifically bound to *MDM2* in a concentration-dependent manner, but did not bind GST, and the binding was significantly reduced by the addition of high concentrations of unconjugated MA242, validating the specificity of the MA242-*MDM2* binding. Further pull-down assays demonstrated that MA242 binds to full-length GST-*MDM2* and GST-*MDM2* (aa 261–491) containing the RING domain (aa 438–479), but not GST-*MDM2* (aa 1–260) containing only the p53 binding domain (p53BD, aa 25–109) or GST-*MDM2* containing only the central domain (aa 180–298) (Fig. 2E), indicating that MA242 directly binds the C-terminal RING domain of *MDM2*. The MA242-*MDM2* binding was further confirmed by cellular thermal shift assays in intact cells. As shown in Fig. 2F, MA242 was quickly and effectively engaged by the *MDM2* protein in both HepG2 and Huh7 cells.

Our molecular docking study with the *NFAT1* DNA binding domain (DBD) (PDB ID: 1OWR) predicted that the 2-amino group of MA242 directly interacts with GLU532 and ASP534 of *NFAT1* via hydrogen bonding (Fig. 2G). Pull-down assays indicated that biotin-MA242 specifically binds to the *NFAT1* DBD, and this was significantly reduced by high concentrations of non-biotinylated MA242, validating the specificity of the MA242-*NFAT1* binding (Fig. 2H). Taken together, these findings demonstrated that MA242 is a specific dual inhibitor of *MDM2* and *NFAT1* with a high binding capacity for both proteins.

3.3. MA242 exerts cytotoxicity against HCC cells by inhibiting the *NFAT1*-*MDM2* pathway in vitro, independent of p53

MA242 was first evaluated for its cytotoxicity against two normal human hepatocyte cell lines, CL48 (p53 wild-type (wt)) and LO2 (p53 wt), and several HCC cell lines, including HepG2 (p53 wt), SMMC-7721 (p53 wt), Huh7 (p53 mutant (mt)), PLC/PRF/5 (p53 mt), MHCC-97H (p53 mt), MHCC-LM3 (p53 mt), and Hep3B (p53 null). As shown in Fig. 3A, MA242 showed selective cytotoxicity against HCC cells, with IC_{50} values ranging from 0.1 to 0.31 μ M. In contrast, this compound had

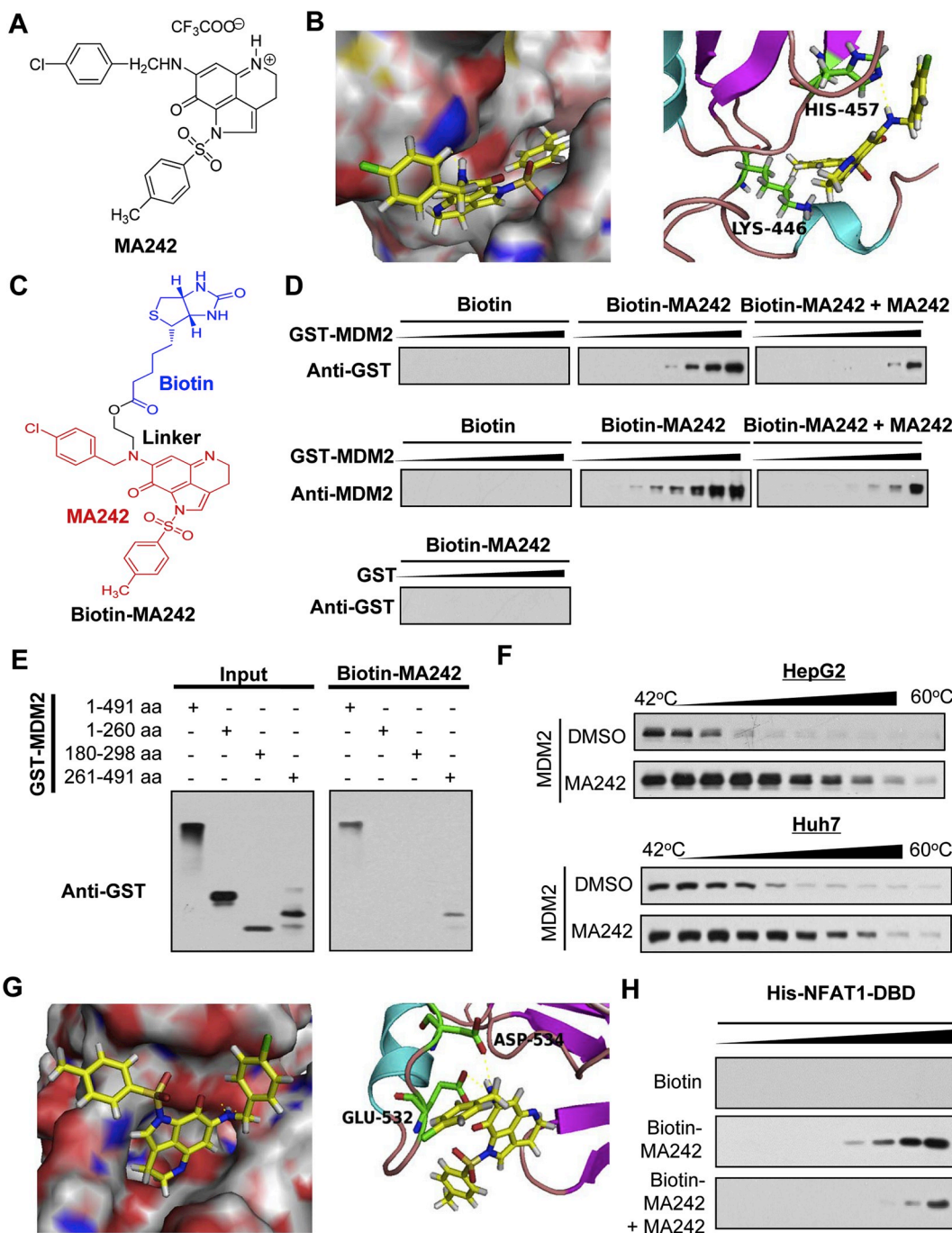


Fig. 2. MA242 directly binds the MDM2 and NFAT1 proteins. (A) The chemical structure of MA242. (B) Molecular docking studies predicts that MA242 directly binds to the C-terminal RING domain of MDM2. The binding site and orientation of MA242 in the C-terminal RING domain of MDM2 (left panel). The protein is the indistinct surface, and MA242 is rendered primarily in yellow. The predicted binding of MA242 with the RING domain of MDM2 is shown in the right panel. Most of MDM2 is rendered in cartoon form, while the residues in contact with MA242 (Lys-446 and His-457) are rendered as sticks. (C) The chemical structure of biotinylated MA242 (Biotin-MA242). (D, E, F) Biological studies confirms that MA242 directly binds to the C-terminal RING domain of MDM2. Biotin-MA242 was incubated with avidin beads, and then incubated with various concentrations of purified (D) GST-MDM2 or (E) various MDM2 deletion proteins in the presence or absence of 10 mM of non-biotinylated MA242. Purified GST was used as a negative control. The bound protein was detected using anti-MDM2 or anti-GST antibodies. (F) HepG2 and Huh7 cells were exposed to 0.5 μ M of MA242 for 3 h, followed by cellular thermal shift assays. The target engagement of MA242 with the MDM2 protein in the cells was detected by Western blotting assays. (G, H) Molecular docking and biological studies predict that MA242 directly binds to the DNA binding domain (DBD) of NFAT1. Most of NFAT1 is rendered in cartoon form, while the residues in contact with MA242 (Glu-532 and Asp 534) are rendered as sticks (G). Biotin-MA242 was incubated with avidin beads, and then incubated with various concentrations of purified His-NFAT1 DBD in the presence or absence of 10 mM of non-biotinylated MA242. Biotin was used as a negative control. The bound protein was detected using an anti-His antibody (H). All experiments were repeated at least three times. (For interpretation of the references to colour in this figure legend, the reader is referred to the Web version of this article.)

minimal cytotoxicity against the two normal hepatocyte cell lines, with IC₅₀ values of 4.75–7.33 μ M. MA242 was also found to inhibit colony formation (Fig. 3B) and cell proliferation (Fig. 3C) in a concentration-

dependent manner in both HepG2 and Huh7 cells. In addition, MA242 induced cell apoptosis (Fig. 3D) and cell cycle arrest (Fig. 3E) at the G₂/M phase in both HepG2 and Huh7 cells. Importantly, MA242

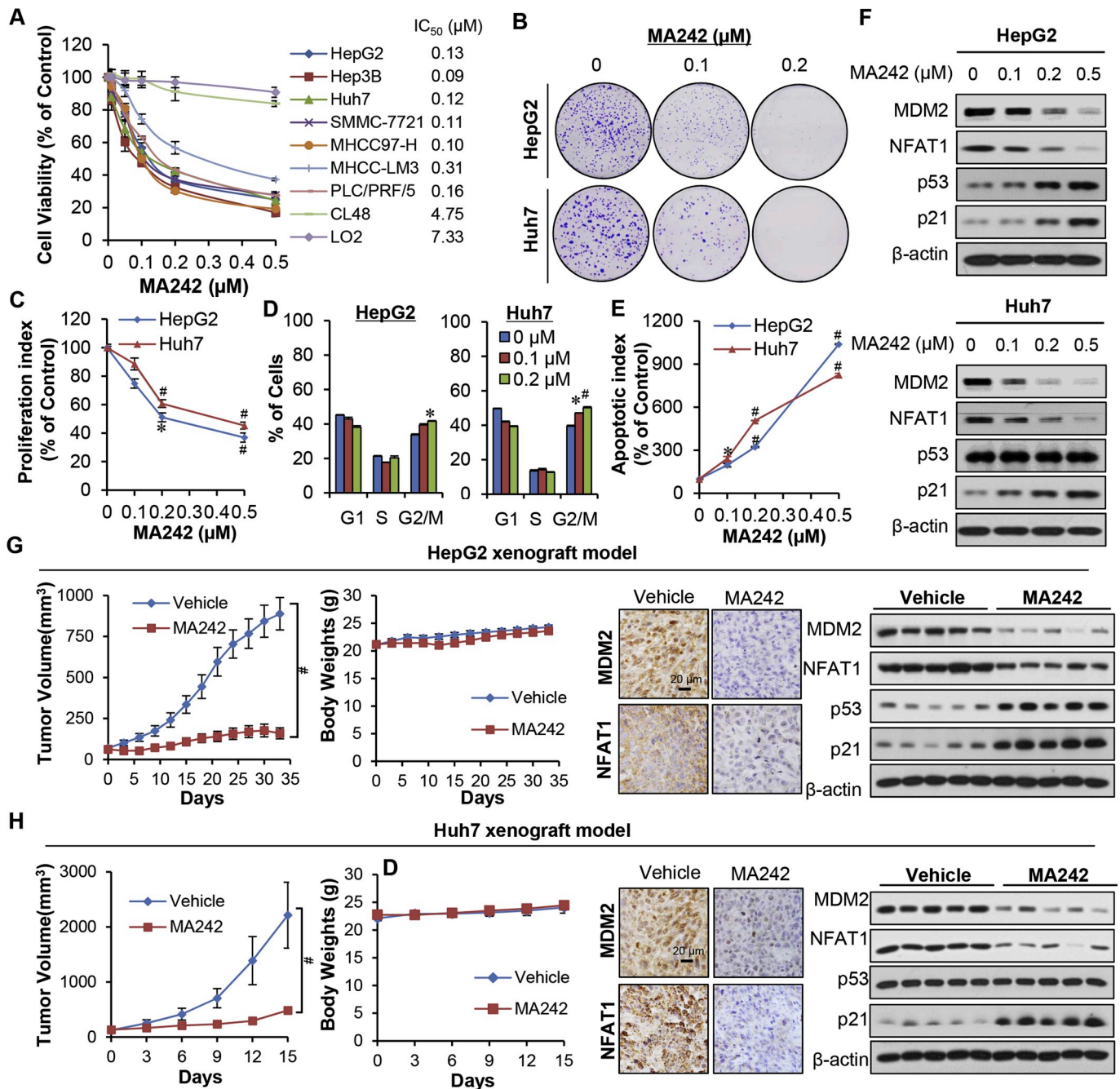


Fig. 3. MA242 inhibits the HCC growth both *in vitro* and *in vivo*, independent of p53. (A) The results of the cell viability assay and the 50% inhibitory concentration (IC₅₀) values of MA242 in normal human hepatocytes (LO2 and CL48) and HCC cell lines. HepG2 and Huh7 cells were exposed to various concentrations of MA242 for 24 h prior to (B) colony formation assays, (C) proliferation assays, (D) cell cycle distribution assays, (E) apoptosis assays, and (F) evaluations of the expression of MDM2, NFAT1, and related proteins. MA242 was administered to nude mice bearing HepG2 (G) or Huh7 (H) xenograft tumors by i.p. injection at a dose of 10 mg/kg/d, 5 d/wk for 33 or 15 days, respectively. Animals were monitored for changes in body weight as a surrogate marker for toxicity in both models. At the end of the experiments, the tumors were excised and analyzed for the expression of proteins of interest by immunohistochemistry (scale bar, 20 μm) and Western blotting assays (each lane represents a different tumor sample). All assays were performed in triplicate and were repeated three times. The data were analyzed by Student's *t*-test and are shown as the means ± SEM. For all graphs: * *P* < 0.05 and # *P* < 0.01.

concentration-dependently decreased the expression levels of both MDM2 and NFAT1, and increased the expression levels of wild-type p53 and p21 (Fig. 3F).

3.4. MA242 suppresses HCC xenograft tumor growth by inhibiting the NFAT-MDM2 pathway *in vivo*, independent of p53

We next examined the *in vivo* efficacy of MA242 in HepG2 and Huh7 xenograft tumor models. As shown in Fig. 3G and H, nude mice bearing

HepG2 and Huh7 xenograft tumors were treated with or without MA242 (10 mg/kg/day, 5 days/week) by intraperitoneal injection for 33 and 15 days, respectively. The choosing of dose for HCC treatment were selected based on our initial Maximum Tolerated Dose (MTD) and safety studies as well as the further optimization for better efficacy and safety. Compared to the control mice, MA242 inhibited tumor growth by 82.1% and 78.1%, respectively. Of note, no remarkable changes were observed in the average body weights of either control or MA242-treated mice, suggesting that there was no major host toxicity induced

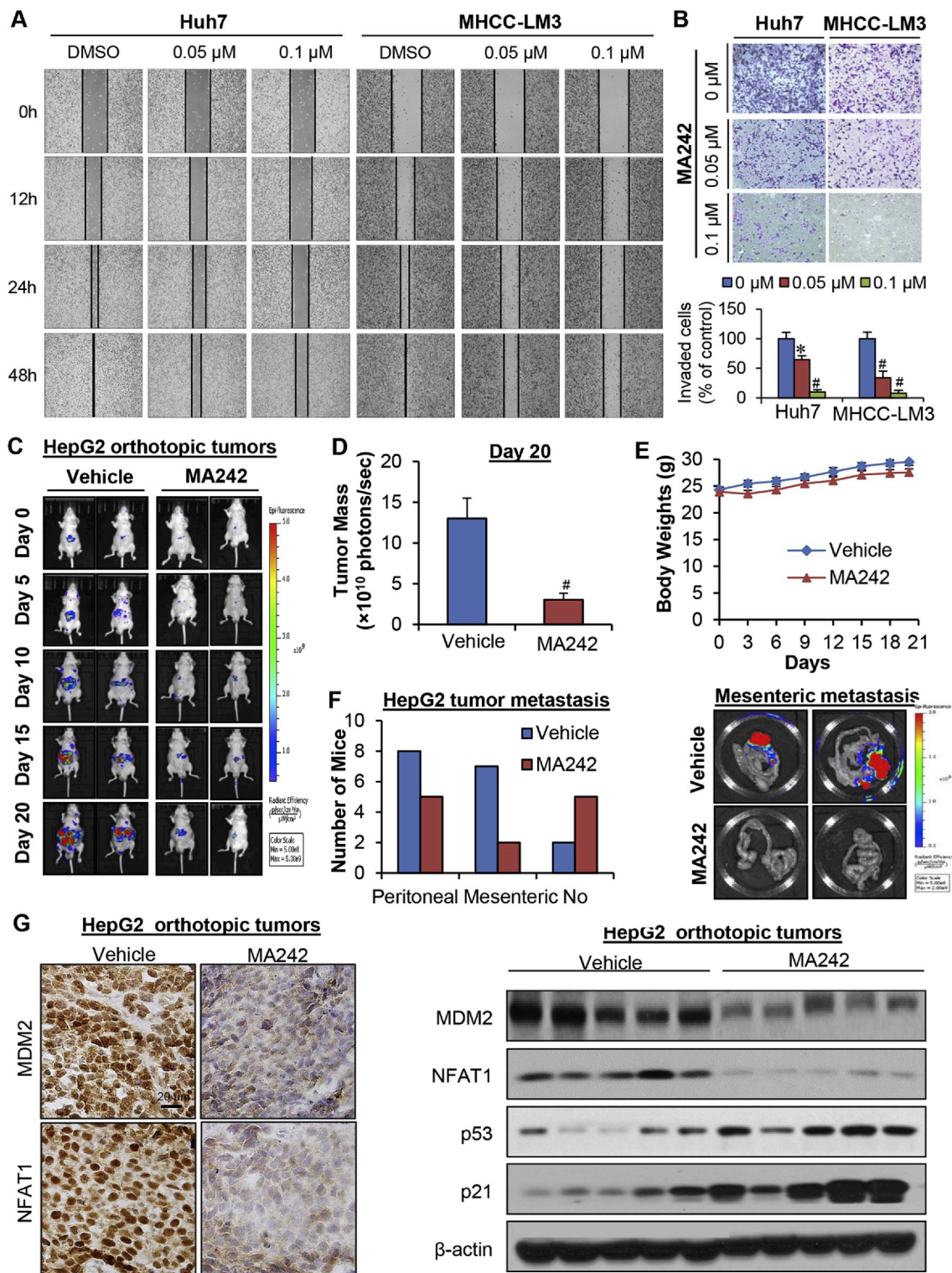


Fig. 4. MA242 inhibits metastasis of HCC both *in vitro* and *in vivo*, independent of p53. Huh7 and MHCC-LM3 cells were exposed to various concentrations (0, 0.05, and 0.1 μ M) of MA242 for 24 h. Then (A) the migration of the cells was measured by wound healing assays and (B) cell invasion was measured using transwell invasion assays. (C) HepG2-GFP cells were implanted orthotopically into the left liver lobe of nude mice. Tumor-bearing mice were randomly grouped and treated with MA242 by i.p. injection at doses of 10 mg/kg/d, 5 d/wk for 20 days. The tumor size was monitored once every 5 days by fluorescence imaging via an IVIS *in vivo* imaging system. (D) On Day 20, the average tumor mass (expressed as photons/sec) of the MA242-treated mice was compared with that of the vehicle control mice. (E) The animals were monitored for changes in body weight as a surrogate marker for toxicity. (F) At the end of the experiments, the numbers of mice with metastasis to the peritoneum and mesentery were counted. Representative images showing mesenteric metastasis are presented. (G) The tumors were excised and analyzed for the expression of MDM2 and NFAT1 by immunohistochemistry (scale bar, 20 μ m) and Western blotting assays (each lane represents a different tumor sample). All assays were performed in triplicate and were repeated three times. The data were analyzed by Student's *t*-test and are shown as the means \pm SEM. For all graphs: * $P < 0.05$ and # $P < 0.01$.

by MA242 (Fig. 3G and H). All tumors were analyzed by immunohistochemistry and Western blot analyses, and the results indicated that the expression levels of both NFAT1 and MDM2 were decreased in MA242-treated tumors. In addition, the expression levels of wild-type p53 (in HepG2 tumors) and p21 were also up-regulated by MA242 *in vivo* (Fig. 3G and H).

3.5. MA242 prevents HCC cell migration and invasion *in vitro* and suppresses metastasis *in vivo*

We further assessed the effects of MA242 on HCC cell migration and invasion. As shown in Fig. 4A, treatment with low concentrations (0.05 and 0.1 μM) of MA242 significantly inhibited the migration of both Huh7 and MHCC-LM3 (a well-documented cell line with high metastatic potential) cells into the wounded areas. Similarly, MA242 concentration-dependently prevented the invasion of both cell lines (Fig. 4B). The *in vivo* efficacy of MA242 was examined in nude mice bearing orthotopic HepG2 tumors (Fig. 4C). MA242 (10 mg/kg/day) was administered by i.p. injection 5 days/week for 20 days, resulting in 76.6% inhibition of tumor growth (Fig. 4D). MA242 did not cause any overt host toxicity at this effective dose, as indicated by the similar average body weights between the vehicle- and MA242-treated mice during the treatment period (Fig. 4E). These results were confirmed by histological examinations of the major organs (liver, lungs, kidneys, spleen, heart, and brain) from these mice (Fig. S3). Importantly, compared with the vehicle-treated mice, MA242 significantly prevented the metastasis of HepG2 tumors to the peritoneum and mesentery, and also decreased the incidence of peritoneal dissemination and mesenteric metastasis from 8/10 and 7/10 to 5/10 and 2/10 animals, respectively (Fig. 4F). Further, the immunohistochemical staining and Western blot analysis of tumor tissues (Fig. 4G) indicated that the MDM2 and NFAT1 protein expression levels were significantly reduced by MA242 *in vivo*. Increased expression of p53 and p21 were also noted in MA242-treated tumors, which was consistent with the *in vitro* observations.

3.6. MA242 promotes MDM2 auto-ubiquitination and protein degradation

The MA242-induced MDM2 inhibition was confirmed by immunofluorescence studies in both the HepG2 and Huh7 cell lines (Fig. 5A). MDM2 protein turnover studies indicated that MA242 decreased the MDM2 protein stability by shortening MDM2's half-life and inducing its proteasomal degradation, protecting wild-type p53 from MDM2-mediated degradation (Fig. 5B and C). Since MDM2 auto-ubiquitination is mainly responsible for its degradation [36], MA242 was examined for its effects on MDM2 ubiquitination. The results indicated that this compound concentration-dependently promoted MDM2 ubiquitination in both HepG2 and Huh7 cells (Fig. 5D). We also observed that MA242 inhibited the expression of wild-type MDM2 and did not induce the degradation of a MDM2 mutant (C464A) lacking ubiquitin E3 ligase activity (Fig. 5E), confirming that MA242 induced MDM2 auto-ubiquitination and protein degradation.

3.7. MA242 inhibits NFAT1-mediated MDM2 transcription

MA242 was further examined for its effects on MDM2 transcription in HCC cells. We first observed that MA242 down-regulated MDM2 mRNA expression, but not p53 mRNA (data not shown) in a concentration-dependent manner in both HepG2 and Huh7 cells (Fig. 6A). MA242 was then assessed for its effects on the MDM2 P1 and P2 promoter activity, and the results indicated that this compound selectively inhibited the MDM2 P2 promoter activity in a concentration-dependent manner, but it had no significant effects on the MDM2 P1 promoter (Fig. 6B). To determine the site on the MDM2 P2 promoter that responded to MA242 treatment, HepG2 and Huh7 cells were transfected with various deletions (Fig. S4) and site mutations of the MDM2 P2 promoter and then exposed to MA242. As shown in Fig. 6C and D, all of

the deletions and mutations of the promoter showed similar responses to MA242 except the construct without the NFAT binding site. NFAT1, but no other NFAT family members, binds to the MDM2 P2 promoter and activates MDM2 transcription [20]. Therefore, we examined the importance of NFAT1 for the MA242-induced repression of MDM2 transcription. The results from an electrophoretic mobility shift assay (EMSA) (Fig. 6E) indicated that MA242 inhibited the binding of both NFAT1 and ionomycin-activated NFAT1 to the MDM2 P2 promoter. These findings were confirmed by a ChIP assay (Fig. 6F).

3.8. MDM2 plays a critical role in MA242-induced anti-HCC activity

To determine whether the inhibition of MDM2 is critical for MA242's anti-cancer activity, we examined the *in vitro* activity of MA242 in MDM2 KO HepG2 and Huh7 cell lines, as well as their corresponding parent cell lines. As shown in Fig. 7A, MDM2 KO by CRISPR/Cas9-mediated editing specifically blocked the effects of MA242 on MDM2 expression. Importantly, CRISPR/Cas9-mediated MDM2 KO reduced the effects of MA242 on cell growth (Fig. 7B). We further observed that MDM2 KO decreased MA242's effects on invasion (Fig. 7C) in cell lines with high metastatic potential, confirming the critical role of MDM2 in the anti-HCC activity of MA242.

To validate the anti-HCC effects of MA242-MDM2 binding, patient-derived HCC xenograft models with different MDM2 expression levels were treated with MA242. Our results showed that MA242 treatment inhibited the growth of HMP412 (MDM2^{high}) and HMP431 (MDM2^{low}) xenograft tumors by about 68.5% ($P < 0.001$) (Fig. 7D) and 24.7% ($P > 0.05$) (Fig. 7E), respectively. To further investigate the mechanism(s) by which MA242 affects tumor growth, we evaluated the expression levels of both MDM2 and NFAT1 in these *in vivo* models after MA242 treatment. Immunohistochemical staining showed that NFAT1 was simultaneously upregulation or downregulation in HMP412 (MDM2^{high}) and HMP431 (MDM2^{low}) xenograft tumors, respectively, treatment with MA242 significantly reduced the expression of both MDM2 and NFAT1 in HMP412 (MDM2^{high}) xenograft tumors, but not in the HMP431 model, indicating that the MDM2 and NFAT1 inhibition induced by MA242 is critical for the anticancer activity of this compound (Fig. 7D and E).

4. Discussion

The present study was designed to develop a dual-targeting (MDM2 and NFAT1) therapeutic strategy for HCC. We have made several important discoveries. First, our results demonstrate that both MDM2 and NFAT1 are frequently overexpressed in HCC tissues in comparison with non-malignant peritumoral tissues. Additionally, the overexpression of MDM2 and NFAT1 is correlated with a poorer prognosis, increased metastasis, and increased tumor aggressiveness. Univariate and multivariate analyses revealed that both the MDM2 and NFAT1 expression levels were independent and significant risk factors for the OS and RFS of patients, indicating that MDM2 and NFAT1 expression can serve as valuable predictors of survival in patients with HCC. Second, the specificity of MA242 as a dual inhibitor of MDM2 and NFAT1 is demonstrated in several assays. We found that it directly bound to the C-terminal RING domain of MDM2 and the DNA binding domain of NFAT1 with high affinity. Moreover, MA242 has two distinct mechanisms of MDM2 inhibition. At the posttranslational level, MA242 increases MDM2 auto-ubiquitination and promotes its proteasomal degradation, independent of p53. At the transcriptional level, MA242 inhibits the binding of the NFAT1 protein to the MDM2 P2 promoter, resulting in repressed MDM2 transcription. MA242 represents a first-in-class MDM2 inhibitor that both promotes MDM2 auto-ubiquitination and degradation and represses NFAT1-mediated MDM2 expression. Third, MA242 potently inhibits HCC cell growth, proliferation, and colony formation, induces G2/M phase arrest and apoptosis, and prevents HCC cell migration and invasion, independent of p53. Fourth,

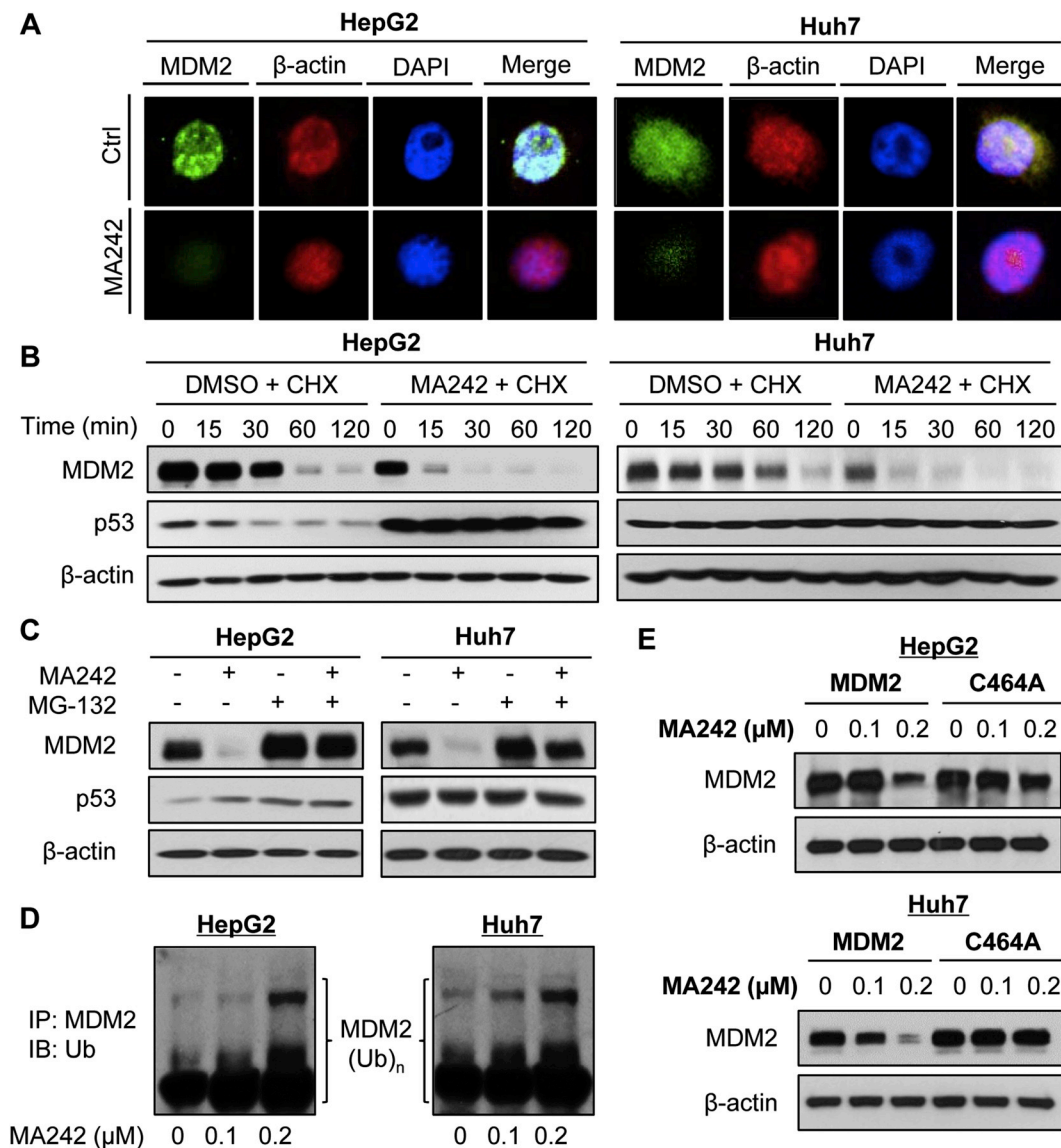


Fig. 5. MA242 promotes MDM2 auto-ubiquitination and protein degradation in HCC cells, independent of p53. (A) Cells were treated with MA242 (0.2 μ M) or vehicle for 6 h, followed by immunofluorescence detection of MDM2 (scale bar, 5 μ m). β -actin and DAPI were used as internal references. (B) The cells were exposed to DMSO or MA242 (0.2 μ M) for 24 h, followed by treatment with a protein synthesis inhibitor, cycloheximide (CHX, 15 μ g/mL). The protein expression levels of MDM2, p53 and β -actin were detected by Western blotting assays at the indicated times after exposure to CHX. (C) The cells were exposed to DMSO or MA242 (0.2 μ M) for 24 h, and then were treated with MG-132 (25 μ M), a proteasome inhibitor, for 6 h. The protein expression levels of MDM2, p53, and β -actin were detected by Western blotting assays. (D) The cells were co-transfected with MDM2 and ubiquitin plasmids, followed by exposure to MA242 (0, 0.1, and 0.2 μ M) for 24 h. Then the cell lysates were subjected to immunoprecipitation with an anti-MDM2 antibody, and the ubiquitinated MDM2 was detected using an anti-ubiquitin antibody. (E) The cells were transfected with a wild-type MDM2 plasmid or a mutant MDM2 plasmid (C464A) without E3 ligase activity, then were treated with MA242 for 24 h. The MDM2 protein levels were detected by Western blotting assays. All assays were performed in triplicate and were repeated three times.

MA242 inhibits MDM2 expression and suppresses tumor growth and metastasis *in vivo*, without inducing any obvious host toxicity. Finally, MDM2 is critical for the MA242-induced anti-HCC activity, and the compound is active regardless of the p53 status of the cells/tumors. In the present study, CRISPR/Cas9-mediated MDM2 KO and a patient-derived xenograft model with low MDM2 expression were used to demonstrate that the MDM2 knockout or knockdown cells were resistant to the compound, showing less sensitivity in terms of their cell growth *in vitro* and *in vivo*. Overall, our results demonstrate that the dual targeting of MDM2 and NFAT1 is an effective and safe strategy for the treatment of HCC, and describe the development of a first-in-class small molecule dual MDM2-NFAT1 inhibitor that can be considered as a candidate for HCC therapy.

The present study includes at least three innovative aspects. First, it represents the first attempt to demonstrate the role of NFAT1-MDM2

signaling in hepatocarcinogenesis. Second, targeting both MDM2 and NFAT1 represents an effective strategy for targeted therapy for HCC. Although MDM2 and NFAT1 have been separately investigated as molecular targets for anticancer drug discovery, targeting both MDM2 and NFAT1 using a single agent is a new concept. Considering that both MDM2 and NFAT1 play pivotal roles in tumor progression and metastasis, simultaneously targeting both pathways will be highly efficient. Third, MA242 is a first-in-class inhibitor with unique mechanisms of action different from those of the existing MDM2 and NFAT1 inhibitors. MA242 directly binds to both the MDM2 and NFAT1 proteins with high affinity and induces their protein degradation; it also inhibits NFAT1-mediated MDM2 transcription via both p53-dependent and -independent mechanisms.

In summary, the present study provides critical information on the clinical relevance of NFAT1 and MDM2 expression in HCC, the value of

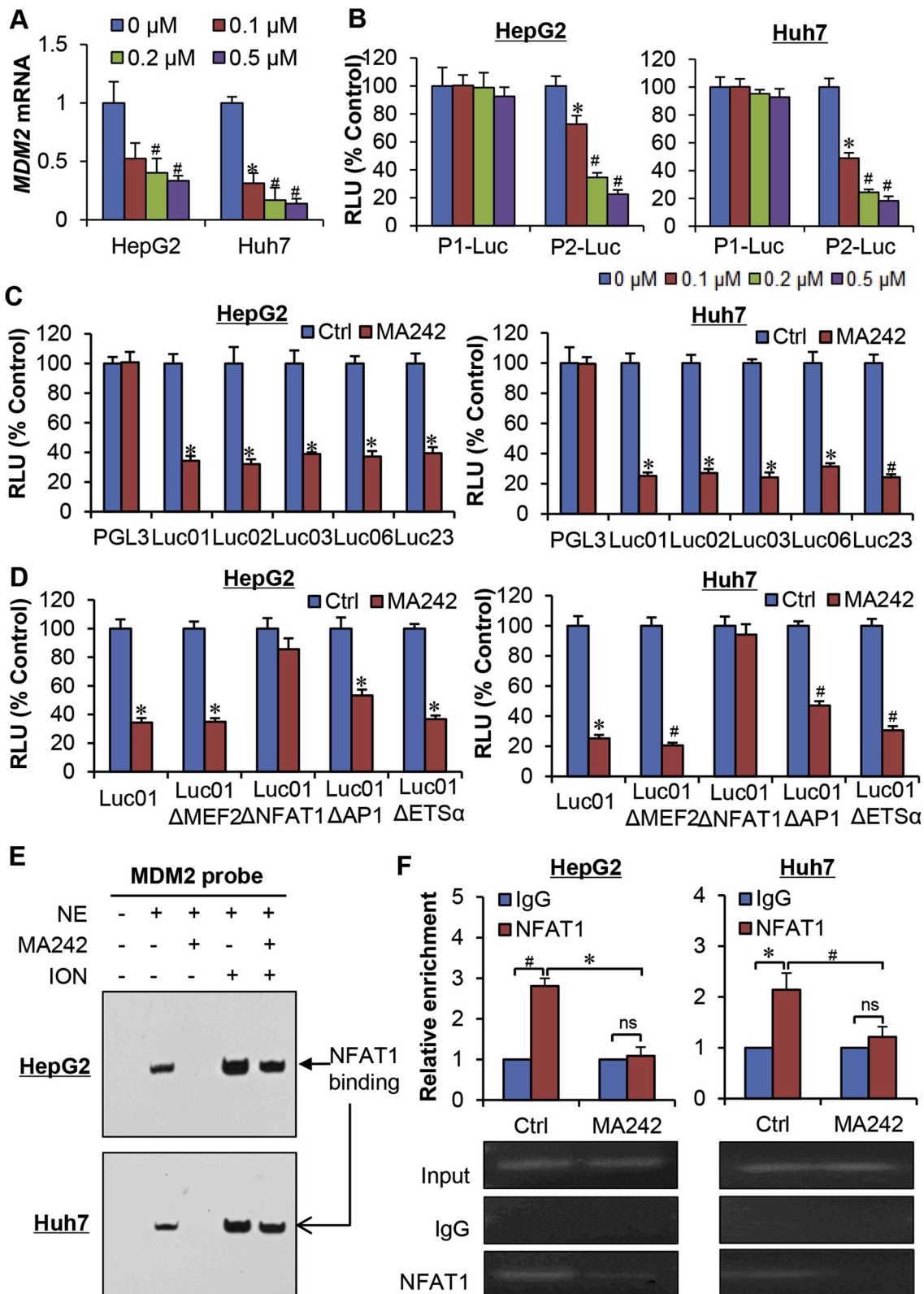


Fig. 6. MA242 inhibits NFAT1-mediated MDM2 transcription in HCC cells, independent of p53. (A) HepG2 and Huh7 cells were exposed to MA242 (0, 0.1, 0.2, and 0.5 μM) for 24 h. The relative *MDM2* mRNA levels were determined by quantitative real-time PCR and normalized to those of *GAPDH* mRNA. (B) The cells were transfected with either *MDM2* P1 promoter luciferase (*MDM2* P1-Luc) or *MDM2* P2 promoter luciferase (*MDM2* P2-Luc) for 12 h. The transfected cells were treated with MA242 (0, 0.1, 0.2, and 0.5 μM) for 24 h, then the luciferase activity was measured. The cells were transfected with (C) full length or deleted *MDM2* P2 promoters or (D) full length or site-mutated *MDM2* P2 promoters for 12 h, followed by exposure to MA242 (0.2 μM) for an additional 24 h before the luciferase activity was measured. (E) The cells were exposed to MA242 (0.2 μM) for 24 h in the presence or absence of ionomycin (ION, 4 μM). Nuclear proteins were extracted and incubated with an *MDM2* probe, followed by an EMSA assay. NE: nuclear extracts. (F) The cells were exposed to MA242 (0.2 μM) for 24 h. Cell lysates were immunoprecipitated with NFAT1 or IgG antibodies, followed by a PCR analysis. All assays were performed in triplicate and were repeated three times. The data were analyzed by Student's *t*-test and are shown as the means ± SEM. For all graphs: **P* < 0.05, #*P* < 0.01, and “ns” denotes “not significant”.

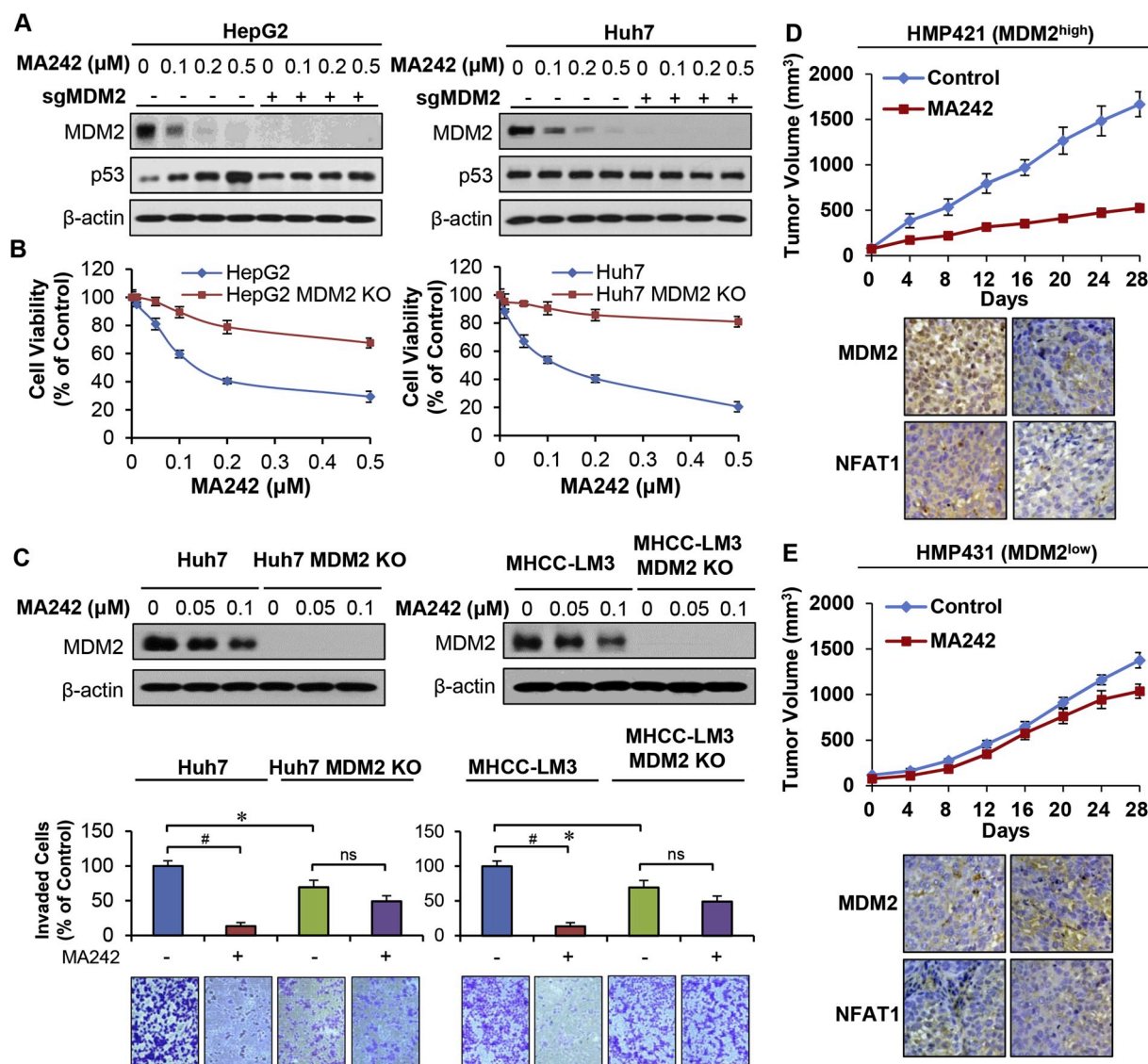


Fig. 7. MDM2 plays a critical role in MA242-induced anti-HCC activity. HepG2 and Huh7 cells with or without CRISPR/Cas9-mediated MDM2 knockout (sgMDM2) were exposed to MA242 (0, 0.1, 0.2, and 0.5 μM) for 24 h or 72 h, followed by (A) Western blot analyses of protein expression or (B) cell viability measurement via MTT assays, respectively. (C) Huh7 and MHCC-LM3 cells with or without MDM2 KO were exposed to MA242 (0.05 μM) for 24 h, then cell invasion was measured using transwell invasion assays. HMP412 (MDM2^{high}) (D) and HMP431 (MDM2^{low}) (E) tumor tissues from patients were implanted into the right flanks of male NOD/SCID mice. MA242 was administered by i.p. injection at doses of 40 mg/kg/d, 5 d/wk for 4 weeks. Upon the termination of the experiments, the tumors were removed and analyzed for the protein expression of MDM2 and NFAT1 by immunohistochemistry (scale bar, 20 μm). All assays were performed in triplicate and were repeated three times. The data were analyzed by Student's *t*-test and are shown as the means \pm SEM. For all graphs: * *P* < 0.05 and # *P* < 0.01.

simultaneously targeting NFAT1 and MDM2, and on the therapeutic efficacy and safety of MA242. The results provide a clinical candidate for HCC therapy and a revolutionary strategy for the development of dual-targeting anticancer agents.

Contributors

Study concept and design: WW, XY, RZ; Acquisition of data: WW, JC, JJQ, BH, XL; Analysis and interpretation of data: WW, JC, JJQ, BH, XL, XY, RZ; Drafting of the manuscript: WW, JC, JJQ, BH, JF, XY, RZ; Statistical analysis: WW, JJQ; Obtained funding: WW, SV, JF, XY, RZ; Administrative, technical, or material support: WW, BN, SV, JF, XY, RZ; Study supervision: WW, XY, RZ.

Conflicts of interest

The authors do not report any conflicts of interest.

Acknowledgements

W.W. and R.Z. were partially supported by National Institutes of Health (NIH)/National Cancer Institute grants (R01 CA186662 and R01CA214019). W.W. and R.Z. were also supported by American Cancer Society (ACS) grant RSG-15-009-01-CDD. R.Z. was partially supported by funds for Robert L. Boblitt Endowed Professor in Drug Discovery and research funds from College of Pharmacy and University of Houston. S.V. was supported by Collaborative Programmatic Development grant 1UL1RR025777 from the UAB Comprehensive Cancer Center and NIH National Center for Research Resources. J.C., J.F., and X-R.Y. were partially supported by grants from the National Natural Science Foundation of China (Nos. 81272389, 81472674, and 81502486). The content is solely the responsibility of the authors, and does not necessarily represent the official views of the National Institutes of Health or other funding agencies. We thank Dr. Elizabeth Rayburn for excellent assistance in the preparation of this manuscript.

Appendix A. Supplementary data

Supplementary data to this article can be found online at <https://doi.org/10.1016/j.canlet.2019.114429>.

References

- [1] R.L. Siegel, K.D. Miller, A. Jemal, Cancer statistics, 2019, *CA Cancer J. Clin.* 69 (2019) 7–34.
- [2] J.D. Yang, L.R. Roberts, Hepatocellular carcinoma: a global view, *Nat. Rev. Gastroenterol. Hepatol.* 7 (2010) 448–458.
- [3] H.B. El-Serag, Hepatocellular carcinoma, *N. Engl. J. Med.* 365 (2011) 1118–1127.
- [4] A.F. Brito, A.M. Abrantes, J.G. Tralhão, et al., Targeting hepatocellular carcinoma: what did we discover so far? *Onco Rev.* 10 (2016) 302.
- [5] J. Bruix, M. Sherman, Management of hepatocellular carcinoma: an update, *Hepatology* 53 (2011) 1020–1022.
- [6] K. Wang, Molecular mechanisms of hepatic apoptosis, *Cell Death Dis.* 5 (2014) e996.
- [7] E. Rayburn, R. Zhang, J. He, et al., MDM2 and human malignancies: expression, clinical pathology, prognostic markers, and implications for chemotherapy, *Curr. Cancer Drug Targets* 5 (2005) 27–42.
- [8] X. Meng, D.A. Franklin, J. Dong, et al., MDM2-p53 pathway in hepatocellular carcinoma, *Cancer Res.* 74 (2014) 7161–7167.
- [9] T. Santarius, J. Shipley, D. Brewer, et al., A census of amplified and overexpressed human cancer genes, *Nat. Rev. Canc.* 10 (2010) 59–64.
- [10] M.F. Zhang, Z.Y. Zhang, J. Fu, et al., Correlation between expression of p53, p21/WAF1, and MDM2 proteins and their prognostic significance in primary hepatocellular carcinoma, *J. Transl. Med.* 7 (2009) 110.
- [11] S. Bohlman, J.J. Manfredi, p53-independent effects of Mdm2, *Subcell. Biochem.* 85 (2014) 235–246.
- [12] A. Bouska, C.M. Eischen, Murine double minute 2: p53-independent roads lead to genome instability or death, *Trends Biochem. Sci.* 34 (2009) 279–286.
- [13] S. Nag, J. Qin, K.S. Srivenugopal, et al., The MDM2-p53 pathway revisited, *J. Biomed. Res.* 27 (2013) 254–271.
- [14] P. Chène, Inhibiting the p53-MDM2 interaction: an important target for cancer therapy, *Nat. Rev. Canc.* 3 (2003) 102–109.
- [15] E.R. Rayburn, S.J. Ezell, R. Zhang, Recent advances in validating MDM2 as a cancer target, *Anti Cancer Agents Med. Chem.* 9 (2009) 882–903.
- [16] S. Nag, X. Zhang, K.S. Srivenugopal, et al., Targeting MDM2-p53 interaction for cancer therapy: are we there yet? *Curr. Med. Chem.* 21 (2014) 553–574.
- [17] S.P. Hussain, J. Schwank, F. Staib, et al., TP53 mutations and hepatocellular carcinoma: insights into the etiology and pathogenesis of liver cancer, *Oncogene* 26 (2007) 2166–2176.
- [18] F. Staib, S.P. Hussain, L.J. Hofseth, et al., TP53 and liver carcinogenesis, *Hum. Mutat.* 21 (2003) 201–216.
- [19] Y. Zhao, A. Aguilar, D. Bernard, et al., Small-molecule inhibitors of the MDM2-p53 protein-protein interaction (MDM2 Inhibitors) in clinical trials for cancer treatment, *J. Med. Chem.* 58 (2015) 1038–1052.
- [20] X. Zhang, Z. Zhang, J. Cheng, et al., Transcription factor NFAT1 activates the mdm2 oncogene independent of p53, *J. Biol. Chem.* 287 (2012) 30468–30476.
- [21] J. Fric, T. Zelante, A.Y. Wong, et al., NFAT control of innate immunity, *Blood* 120 (2012) 1380–1389.
- [22] M. Mancini, A. Toker, NFAT proteins: emerging roles in cancer progression, *Nat. Rev. Canc.* 9 (2009) 810–820.
- [23] M.R. Muller, A. Rao, NFAT, immunity and cancer: a transcription factor comes of age, *Nat. Rev. Immunol.* 10 (2010) 645–656.
- [24] J.J. Qin, S. Nag, W. Wang, et al., NFAT as cancer target: mission possible? *Biochim. Biophys. Acta* 1846 (2014) 297–311.
- [25] W. Wang, J. Cheng, J.J. Qin, et al., RYBP expression is associated with better survival of patients with hepatocellular carcinoma (HCC) and responsiveness to chemotherapy of HCC cells in vitro and in vivo, *Oncotarget* 5 (2014) 11604–11619.
- [26] H. Jin, C. Wang, G. Jin, et al., Regulator of calcineurin 1 gene isoform 4, down-regulated in hepatocellular carcinoma, prevents proliferation, migration, and invasive activity of cancer cells and metastasis of orthotopic tumors by inhibiting nuclear translocation of NFAT1, *Gastroenterology* 153 (2017) 799–811.
- [27] J. Ji, Y. Yin, H. Ju, et al., Long non-coding RNA Lnc-Tim3 exacerbates CD8 T cell exhaustion via binding to Tim-3 and inducing nuclear translocation of Bat3 in HCC, *Cell Death Dis.* 9 (2018) 478.
- [28] W. Wang, J.J. Qin, S. Voruganti, et al., The pyrido[b]indole MDM2 inhibitor SP-141 exerts potent therapeutic effects in breast cancer models, *Nat. Commun.* 5 (2014) 5086.
- [29] W. Wang, J.J. Qin, S. Voruganti, et al., Identification of a new class of MDM2 inhibitor that inhibits growth of orthotopic pancreatic tumors in mice, *Gastroenterology* 147 (2014) 893–902.
- [30] W. Wang, J.J. Qin, S. Voruganti, et al., Identification of a new class of natural product MDM2 inhibitor: in vitro and in vivo anti-breast cancer activities and target validation, *Oncotarget* 6 (2015) 2623–2640.
- [31] Y. Li, Z.Y. Tang, S.L. Ye, et al., Establishment of cell clones with different metastatic potential from the metastatic hepatocellular carcinoma cell line MHCC97, *World J. Gastroenterol.* 7 (2001) 630–636.
- [32] Y. Li, Y. Tang, L. Ye, et al., Establishment of a hepatocellular carcinoma cell line with unique metastatic characteristics through in vivo selection and screening for metastasis-related genes through cDNA microarray, *J. Cancer Res. Clin. Oncol.* 129 (2003) 43–51.
- [33] P.D. Hsu, E.S. Land, F. Zhang, et al., Development and applications of applications of CRISPR-Cas9 for genome engineering, *Cell* 157 (2014) 1262–1278.
- [34] M. Li, Z. Zhang, D.L. Hill, et al., Genistein, a dietary isoflavone, down-regulates the MDM2 oncogene at both transcriptional and posttranslational levels, *Cancer Res.* 65 (2005) 8200–8208.
- [35] D. Nicolle, M. Fabre, M. Simon-Coma, et al., Patient-derived mouse xenografts from pediatric liver cancer predict tumor recurrence and advise clinical management, *Hepatology* 64 (2016) 1121–1135.
- [36] S. Fang, J.P. Jensen, R.L. Ludwig, et al., Mdm2 is a RING finger-dependent ubiquitin protein ligase for itself and p53, *J. Biol. Chem.* 275 (2000) 8945–8951.